MOCABA: a general Monte Carlo-Bayes procedure for improved predictions of integral functions of nuclear data

A. Hoefer[a], O. Buss[a], M. Hennebach[a], M. Schmid[a], D. Porsch[b]

[a] *AREVA GmbH – Dep. Radiology & Criticality*
Kaiserleistrasse 29, 63067 Offenbach am Main, Germany
[b] *AREVA GmbH – Dep. Neutronics*
Paul-Gossen-Strasse 100, 91052 Erlangen, Germany

arXiv:1411.3172v1 [nucl-th] 12 Nov 2014

Abstract

MOCABA is a combination of Monte Carlo sampling and Bayesian updating algorithms for the prediction of integral functions of nuclear data, such as reactor power distributions or neutron multiplication factors. Similarly to the established Generalized Linear Least Squares (GLLS) methodology, MOCABA offers the capability to utilize integral experimental data to reduce the prior uncertainty of integral observables. The MOCABA approach, however, does not involve any series expansions and, therefore, does not suffer from the breakdown of first-order perturbation theory for large nuclear data uncertainties. This is related to the fact that, in contrast to the GLLS method, the updating mechanism within MOCABA is applied directly to the integral observables without having to "adjust" any nuclear data. A central part of MOCABA is the nuclear data Monte Carlo program NUDUNA, which performs random sampling of nuclear data evaluations according to their covariance information and converts them into libraries for transport code systems like MCNP or SCALE. What is special about MOCABA is that it can be applied to any integral function of nuclear data, and any integral measurement can be taken into account to improve the prediction of an integral observable of interest. In this paper we present two example applications of the MOCABA framework: the prediction of the neutron multiplication factor of a water-moderated PWR fuel assembly based on 21 criticality safety benchmark experiments and the prediction of the power distribution within a toy model reactor containing 100 fuel assemblies.

Keywords: uncertainty analysis, nuclear data, Monte Carlo methods, nuclear criticality safety, reactor analysis

1. Introduction

Over the last years, methods of Monte Carlo propagation of nuclear data uncertainties have been playing an increasingly important role in the uncertainty analysis of integral observables, such as neutron multiplication factors, isotopic concentrations in irradiated nuclear fuel or reactor power distributions (Koning and Rochman, 2008; Sanz et al., 2008; Zwermann et al., 2010; Buss et al., 2011; Williams et al., 2012; Wieselquist et al., 2013). This is largely owed to the fact that comprehensive covariance data have been added to the major nuclear data evaluations (Chadwick et al., 2011; Shibata et al., 2011; JEFF team, 2014; Koning and Rochman, 2011). The application range of Monte Carlo based nuclear data uncertainty propagation is very wide and extends from criticality safety analysis over reactor core analysis, depletion analysis and activation analysis to more exotic applications like the design of accelerator-driven systems and fusion systems (Buss et al., 2011; Williams et al., 2012; Klein et al., 2012; Pasichnyk et al., 2012; Garcia-Herranz et al., 2008; Diez et al., 2013; Rochman et al., 2011a).

Email address: axel.hoefer@areva.com (A. Hoefer)

However, the traditional way of propagating nuclear data uncertainties is *not* based on Monte Carlo simulation but on adjoint-based first-order perturbation theory, where uncertainties of integral observables due to nuclear data uncertainties are approximated by linear transformations of nuclear data covariances. These linear transformations are defined by the sensitivities of the integral observables to the nuclear data (Uchasev, 1964; Gandini, 1967; Broadhead et al., 2004).

A major strength of first-order perturbation theory is that it can be combined with the Generalized Linear Least Squares (GLLS) method, which allows us to utilize integral experimental data to update prior knowledge about the nuclear data and, consequently, about integral functions of the nuclear data (Cecchini et al., 1965; Humi et al., 1965; Hemment and Pendleburry, 1966; Broadhead et al., 2004; De Saint Jean et al., 2011; Salvatores et al., 2013). This procedure is also often referred to as "nuclear data adjustment".

In spite of the merits of first-order perturbation theory, there are limitations to its applicability:

- If nuclear data uncertainties are too large, first-order perturbation theory breaks down. This may already happen for nuclear data uncertainties in the range

of only a few percent (Hoefer et al., 2011; Rochman et al., 2011b).

- Application cases with a very large number of responses, such as time-dependent pin-wise fission rates in a depletion analysis, would require an unmanageably large number of adjoint transport calculations (Williams et al., 2012).
- Many transport codes do not offer the option to perform adjoint calculations. Adjoint-based first-order perturbation theory is not applicable in such cases (Williams et al., 2012).

Fortunately, the above limitations do not apply to the Monte Carlo propagation of nuclear data uncertainties. An apparent disadvantage of the Monte Carlo approach, however, is that it cannot be combined with GLLS updating. Hence, what we need is a Bayesian procedure similar to the GLLS method which allows us to take into account integral benchmark measurements to update the Monte Carlo predictions of the integral observables of interest.

Such a Bayesian updating mechanism for Monte Carlo data is the main characteristics of the MOCABA approach.

The MOCABA procedure is divided into two steps: a Monte Carlo step and an updating step. In the Monte Carlo step, nuclear data and system parameters defining the application case (e.g. a reactor core) are random sampled from their respective uncertainty distributions. These random draws are then used as input to transport calculations, which provides a multivariate data set of integral observables for the application case and the benchmark experiments. In the updating step, information related to the benchmark experiments is added, namely the integral measurements as well as the system parameters defining the experimental setups and their uncertainties. This provides us with updated estimates and uncertainties of the integral observables for the benchmark experiments *and* with updated predictions and uncertainties of integral observables for the application case. Constraints on linear combinations of the integral observables (e.g. a constraint on the total power of a nuclear reactor) may also be included in the updating step.

Depending on the degree of physical similarity between the benchmark experiments and the application case[1], the MOCABA approach allows for significantly more precise predictions of integral observables than a Monte Carlo approach without Bayesian updating. This makes MOCABA very useful for a lot of applications.

One of the merits of the MOCABA framework is that it can be applied to any function of nuclear data, including vectors of local power values defining the power distributions within nuclear reactors, vectors of isotopic concentrations defining the compositions of irradiated fuel samples, or individual neutron multiplication factors. Moreover, any integral measurement can be used as a benchmark for the updating procedure. We may even include measurements of integral observables that seem very different from those we want to predict, like reactor power measurements as benchmarks for the prediction of the isotopic composition of a completely unrelated irradiated fuel assembly.

In the following, we first present a description of the statistical model and its implementation. The MOCABA procedure is then applied to the prediction of the neutron multiplication factor of a water-moderated PWR fuel assembly and to the prediction of the power distribution within a toy model reactor. We conclude the paper with a short summary and outlook.

2. The Bayesian model and its implementation

2.1. Definition of the Bayesian model

Let us consider an arbitrary vector function $\mathbf{y}$ of a nuclear data vector $\boldsymbol{\alpha}$:

$$\mathbf{y}(\boldsymbol{\alpha}) = (y_1(\boldsymbol{\alpha}), \ldots, y_n(\boldsymbol{\alpha}))^T, \quad \boldsymbol{\alpha} = (\alpha_1, \ldots, \alpha_r)^T. \quad (1)$$

To express nuclear data uncertainties, $\boldsymbol{\alpha}$ is treated as a random vector defined by an r-variate probability density function (pdf) $\mathrm{p}(\boldsymbol{\alpha})$. Consequently, $\mathbf{y}(\boldsymbol{\alpha})$ as a function of $\boldsymbol{\alpha}$ is also a random vector defined by an n-variate pdf $\mathrm{p}(\mathbf{y})$ which reflects the uncertainty of $\mathbf{y}$ due to nuclear data uncertainties. $\mathrm{p}(\mathbf{y})$ is identified with an n-variate normal distribution defined by a mean vector $\mathbf{y}_0$ and a covariance matrix $\boldsymbol{\Sigma}_0$:[2]

$$\begin{aligned} \mathrm{p}(\mathbf{y}) &= \mathrm{N}(\mathbf{y}_0, \boldsymbol{\Sigma}_0) \propto \exp(-Q_0/2), \\ Q_0 &= (\mathbf{y} - \mathbf{y}_0)^T \boldsymbol{\Sigma}_0^{-1} (\mathbf{y} - \mathbf{y}_0). \end{aligned} \quad (2)$$

Since $\mathrm{p}(\mathbf{y})$ reflects our knowledge about $\mathbf{y}$ before any measurements of $\mathbf{y}$ or constraints on $\mathbf{y}$ are taken into account, we refer to $\mathrm{p}(\mathbf{y})$ as the prior pdf of $\mathbf{y}$.

Measurements of $\mathbf{y}$ and linear constraints on $\mathbf{y}$ may both be expressed in terms of a likelihood function of the following type:

$$\begin{aligned} \mathrm{p}(\mathbf{v} \,|\, \mathbf{y}) &\propto \exp(-Q_V/2), \\ Q_V &= \boldsymbol{\Delta}^T \boldsymbol{\Sigma}_V^{-1} \boldsymbol{\Delta}, \quad \boldsymbol{\Delta} := \mathbf{U}\mathbf{y} - \mathbf{v}. \end{aligned} \quad (3)$$

Here $\mathbf{U}$ is a rectangular matrix, i.e. $\mathbf{U}\mathbf{y}$ represents a linear transformation of $\mathbf{y}$, and $\mathbf{v}$ is a vector defining the measurements and/or linear constraints. Hence, $\mathbf{v}$ represents

[1] Here physical similarity is meant in the sense that two systems are similar if their integral observables have similar sensitivities to variations in the nuclear data.

[2] In case the normality assumption does not hold, e.g. for nonlinear responses of $\mathbf{y}$ to variations in the nuclear data $\boldsymbol{\alpha}$, $\mathbf{y}$ may be mapped onto an approximately normally distributed vector $\mathbf{z}$ by means of an invertible variable transformation f. In that way $\mathrm{p}(\mathbf{y})$ may be chosen from a more general class of distribution models such that the response of $\mathbf{y}$ to variations in $\boldsymbol{\alpha}$ is correctly reflected. The normal Bayesian model described below then applies to the transformed vector $\mathbf{z}$, and the distribution of $\mathbf{y}$ is obtained simply by applying the inverse transformation f^{-1} to $\mathbf{z}$.

the best estimate of $\mathbf{U}\mathbf{y}$ and $\mathbf{\Sigma}_V$ is the corresponding covariance matrix.

According to Bayes' theorem, the updated information about $\mathbf{y}$, which includes the prior knowledge related to the nuclear data as well as the integral measurements and constraints, is represented by the posterior pdf, which is defined as the normalized product of the prior pdf and the likelihood function (Gelman et al., 1998):

$$\mathrm{p}(\mathbf{y}\,|\,\mathbf{v}) \;\propto\; \mathrm{p}(\mathbf{v}\,|\,\mathbf{y})\,\mathrm{p}(\mathbf{y})\,. \tag{4}$$

Since both $\mathrm{p}(\mathbf{y})$ and $\mathrm{p}(\mathbf{v}\,|\,\mathbf{y})$ are multivariate normal, Eq. (4) yields a multivariate normal posterior pdf:

$$\begin{aligned}\mathrm{p}(\mathbf{y}\,|\,\mathbf{v}) \;&=\; \mathrm{N}\,(\mathbf{y}^*, \mathbf{\Sigma}^*) \;\propto\; \exp\,(-Q^*/2)\,,\\ Q^* \;&=\; Q_0 + Q_V \;=\; (\mathbf{y}-\mathbf{y}^*)^T\,\mathbf{\Sigma}^{*-1}\,(\mathbf{y}-\mathbf{y}^*)\,.\end{aligned} \tag{5}$$

Here $\mathbf{y}^*$ is the maximum-a-posteriori estimate and $\mathbf{\Sigma}^*$ the related posterior covariance matrix of $\mathbf{y}$.

To distinguish between observables related to the application case and observables related to the benchmark experiments, $\mathbf{y}$ may be partitioned into an application case vector $\mathbf{y}_A$ and a benchmark vector $\mathbf{y}_B$:

$$\mathbf{y} \;=\; \left(\mathbf{y}_A^T, \mathbf{y}_B^T\right)^T. \tag{6}$$

Accordingly, we also express the model parameters of the prior distribution, the likelihood function and the posterior distribution in partitioned form:

$$\begin{aligned}\mathbf{y}_0 \;&=\; \left(\mathbf{y}_{0A}^T, \mathbf{y}_{0B}^T\right)^T,\;\; \mathbf{\Sigma}_0 \;=\; \begin{pmatrix}\mathbf{\Sigma}_{0A} & \mathbf{\Sigma}_{0AB}\\ \mathbf{\Sigma}_{0AB}^T & \mathbf{\Sigma}_{0B}\end{pmatrix},\\ \mathbf{v} \;&=\; \left(\mathbf{v}_A^T, \mathbf{v}_B^T\right)^T,\quad \mathbf{\Sigma}_V \;=\; \begin{pmatrix}\mathbf{\Sigma}_{VA} & \mathbf{0}\\ \mathbf{0}^T & \mathbf{\Sigma}_{VB}\end{pmatrix},\\ \mathbf{U} \;&=\; \begin{pmatrix}\mathbf{U}_A & \mathbf{0}\\ \mathbf{0}^T & \mathbf{U}_B\end{pmatrix},\;\; \mathbf{y}^* \;=\; \left(\mathbf{y}_A^{*T}, \mathbf{y}_B^{*T}\right)^T,\\ \mathbf{\Sigma}^* \;&=\; \begin{pmatrix}\mathbf{\Sigma}_A^* & \mathbf{\Sigma}_{AB}^*\\ \mathbf{\Sigma}_{AB}^{*T} & \mathbf{\Sigma}_B^*\end{pmatrix}.\end{aligned} \tag{7}$$

To obtain the posterior distribution model parameters $\mathbf{y}^*$ and $\mathbf{\Sigma}^*$, the quadratic form Q^* defined in Eqs. (2), (3) and (5) has to be minimized with respect to $\mathbf{y}$. For cases with direct measurements of each component of $\mathbf{y}_B$ without constraints, which are represented by

$$\mathbf{\Sigma}_{VA}^{-1} \;=\; \mathbf{0},\quad \mathbf{U}_B \;=\; \mathbf{I}, \tag{8}$$

we get the following expressions for the posterior model parameters:

$$\begin{aligned}\mathbf{y}_A^* \;&=\; \mathbf{y}_{0A} + \mathbf{\Sigma}_{0AB}\,(\mathbf{\Sigma}_{0B} + \mathbf{\Sigma}_{VB})^{-1}\,(\mathbf{v}_B - \mathbf{y}_{0B})\,,\\ \mathbf{y}_B^* \;&=\; \mathbf{y}_{0B} + \mathbf{\Sigma}_{0B}\,(\mathbf{\Sigma}_{0B} + \mathbf{\Sigma}_{VB})^{-1}\,(\mathbf{v}_B - \mathbf{y}_{0B})\,,\\ \mathbf{\Sigma}_A^* \;&=\; \mathbf{\Sigma}_{0A} - \mathbf{\Sigma}_{0AB}\,(\mathbf{\Sigma}_{0B} + \mathbf{\Sigma}_{VB})^{-1}\,\mathbf{\Sigma}_{0AB}^T,\\ \mathbf{\Sigma}_B^* \;&=\; \mathbf{\Sigma}_{0B} - \mathbf{\Sigma}_{0B}\,(\mathbf{\Sigma}_{0B} + \mathbf{\Sigma}_{VB})^{-1}\,\mathbf{\Sigma}_{0B},\\ \mathbf{\Sigma}_{AB}^* \;&=\; \mathbf{\Sigma}_{0AB} - \mathbf{\Sigma}_{0AB}\,(\mathbf{\Sigma}_{0B} + \mathbf{\Sigma}_{VB})^{-1}\,\mathbf{\Sigma}_{0B}\,.\end{aligned} \tag{9}$$

As follows from Eq. (9), our knowledge about the application case observables $\mathbf{y}_A$ can be increased by measurements of the benchmark observables $\mathbf{y}_B$, since $\mathbf{y}_A$ and $\mathbf{y}_B$ are correlated by common nuclear data uncertainties. These correlations are represented by the submatrix $\mathbf{\Sigma}_{0AB}$ of the prior covariance matrix $\mathbf{\Sigma}_0$. If the physical characteristics of the application case are very different from those of the benchmark experiments, the components of $\mathbf{\Sigma}_{0AB}$ tend to be very small. Measurements of $\mathbf{y}_B$ then only have a very small impact on our knowledge about $\mathbf{y}_A$, i.e. the posterior estimates $\mathbf{y}_A^*$ and $\mathbf{\Sigma}_A^*$ differ only very little from the prior estimates $\mathbf{y}_{0A}$ and $\mathbf{\Sigma}_{0A}$. Conversely, for benchmark experiments with a very high degree of physical similarity to the application case, the correlations corresponding to $\mathbf{\Sigma}_{0AB}$ are close to one, in which case measurements of the benchmark observables $\mathbf{y}_B$ may significantly improve our knowledge about $\mathbf{y}_A$.

Up to this point, our Bayesian model takes into account nuclear data uncertainties, reflected by the prior covariance matrix $\mathbf{\Sigma}_0$, as well as uncertainties related to the benchmark experiments and constraints, reflected by the likelihood covariance matrix $\mathbf{\Sigma}_V$. What is still missing are the system parameter uncertainties related to the application case. They can, however, be included very easily into the prior pdf $\mathrm{p}(\mathbf{y})$. For this purpose, the parameter vector $\mathbf{x}_A$ characterizing the system parameters of the application case is treated as a random vector defined by a pdf $\mathrm{p}(\mathbf{x}_A)$, and the integral observable vector $\mathbf{y}$ is now considered to be a vector function of the nuclear data random vector $\boldsymbol{\alpha}$ *and* the system parameter random vector $\mathbf{x}_A$:

$$\mathbf{y} \;=\; \mathbf{y}(\boldsymbol{\alpha}, \mathbf{x}_A) \;=\; \left(\mathbf{y}_A^T(\boldsymbol{\alpha}, \mathbf{x}_A), \mathbf{y}_B^T(\boldsymbol{\alpha})\right)^T. \tag{10}$$

Consequently, the prior pdf $\mathrm{p}(\mathbf{y})$ in Eq. (2) is now defined by the pdf $\mathrm{p}(\boldsymbol{\alpha})$ reflecting the nuclear data uncertainties *and* the pdf $\mathrm{p}(\mathbf{x}_A)$ reflecting the system parameter uncertainties of the application case. Hence, the prior distribution model parameters $\mathbf{y}_0$ and $\mathbf{\Sigma}_0$ now represent both the prior information about the nuclear data *and* the information about the system parameters of the application case. Since the parametric structure of the prior pdf is not changed by including system parameter uncertainties of the application case, the procedure of calculating the posterior pdf $\mathrm{p}(\mathbf{y}\,|\,\mathbf{v})$ stays the same as described above.

Having included system parameter uncertainties of the application case into our Bayesian model, the list of uncertainties to be considered is complete.

2.2. The MOCABA procedure

MOCABA is a software implementation of the Bayesian model defined above.

In order to propagate nuclear data uncertainties to integral observable uncertainties, random sampling of ENDF-6-formatted nuclear data files is performed with the aid of the nuclear data Monte Carlo program NUDUNA (Buss et al., 2011) using the uncertainty information included

in the corresponding covariance files of the respective nuclear data evaluation (Chadwick et al., 2011; Shibata et al., 2011; JEFF team, 2014; Koning and Rochman, 2011). NUDUNA is designed to read input data provided in ENDF-6 format CSEWG (2013). Its random sampling is based on the information provided in the File 31-34 uncertainty sections and in File 8 of an ENDF-6 tape, i.e. it considers uncertainties of neutron multiplicities, resonance parameters, cross sections, angular distributions, half-lives, and decay branching ratios. Neutron fission spectrum uncertainties, fission yield uncertainties and correlations of different isotopes are not yet included in the current NUDUNA version. The sampled nuclear data files are subsequently converted automatically into libraries for transport calculations.

The current version of NUDUNA has the capability to generate random ACE tapes for continuous energy transport calculations with MCNP or SERPENT as well as 44-group and 238-group AMPX tapes for transport calculations with SCALE (X-5 Monte Carlo Team, 2003; Leppänen, 2013; Oak Ridge National Laboratory, 2009). To extend the application range to reactor core design and reactor safety analysis, the option to generate few-group libraries for reactor core simulation systems will be included in future versions of NUDUNA.

To take system parameter uncertainties of the application case into account, for each random sample $\boldsymbol{\alpha}_i^{MC}$ of the nuclear data evaluation vector $\boldsymbol{\alpha}$ generated by NUDUNA, a random sample $\mathbf{x}_{A,i}^{MC}$ of the application case system parameter vector $\mathbf{x}_A$ is drawn. The Monte Carlo samples are then used as input parameters for transport calculations of the application case and benchmark observables represented by the components of the integral observable vector $\mathbf{y}$; see Eq. (10). Hence, a set of m random draws of $\boldsymbol{\alpha}$ and $\mathbf{x}_A$ yields a multivariate data set

$$\begin{aligned} Y_{MC} &= \left\{\mathbf{y}_1^{MC}, \ldots, \mathbf{y}_m^{MC}\right\} \\ &= \left\{\mathbf{y}\left(\boldsymbol{\alpha}_1^{MC}, \mathbf{x}_{A,1}^{MC}\right), \ldots, \mathbf{y}\left(\boldsymbol{\alpha}_m^{MC}, \mathbf{x}_{A,m}^{MC}\right)\right\} \end{aligned} \quad (11)$$

of m random draws of $\mathbf{y}$. These data are used for the estimation of the prior pdf $\mathrm{p}(\mathbf{y})$, where we apply the following consistent and unbiased estimators of the prior mean vector and the prior covariance matrix (Gelman et al., 1998):

$$\begin{aligned} \hat{\mathbf{y}}_0 &= \frac{1}{m}\sum_{i=1}^{m}\mathbf{y}_i^{MC}, \\ \hat{\boldsymbol{\Sigma}}_0 &= \frac{1}{m-1}\sum_{i=1}^{m}\left(\mathbf{y}_i^{MC}-\hat{\mathbf{y}}_0\right)\left(\mathbf{y}_i^{MC}-\hat{\mathbf{y}}_0\right)^T. \end{aligned} \quad (12)$$

If a sufficiently large value for the Monte Carlo sample size m is chosen, $\hat{\mathbf{y}}_0$ and $\hat{\boldsymbol{\Sigma}}_0$ may be identified with the prior distribution model parameters $\mathbf{y}_0$ and $\boldsymbol{\Sigma}_0$; see Eq. (2). If the Monte Carlo data Y_{MC} do not fit the assumption that $\mathbf{y}$ is normally distributed, e.g., if there is a strongly nonlinear response of $\mathbf{y}$ to variations in the nuclear data, we can make use of a suitable invertible variable transformation $\mathbf{y} \rightarrow \mathbf{z}$ onto an approximately normally distributed random vector $\mathbf{z}$ (see footnote 2).

Before performing the Bayesian updating according to Eq. (4), we have to translate the benchmark uncertainties into the covariance matrix $\boldsymbol{\Sigma}_V$ of the likelihood function $\mathrm{p}(\mathbf{v}\,|\,\mathbf{y})$; see Eq. (3). For direct measurements of the benchmark observables without any constraints (see Eq. (8)), the measurement vector $\mathbf{v}_B$ is our best estimate of $\mathbf{y}_B$ if we ignore the prior knowledge about the nuclear data, and the covariances of the benchmark measurements due to uncertainties in the benchmark system parameters are represented by the covariance matrix $\boldsymbol{\Sigma}_{VB}$; see Eq. (7).

Collecting the system parameters characterizing all benchmark experiments under consideration into a single parameter vector $\mathbf{x}_B$ allows us to express the benchmark system parameter uncertainties by treating $\mathbf{x}_B$ as a random vector defined by a pdf $\mathrm{p}(\mathbf{x}_B)$. The benchmark measurements are then expressed as a vector function $\mathbf{y}_B(\mathbf{x}_B)$ of this random vector. Since we are generally dealing with sets of measurements that are related by common boundary conditions, like sets of local reactor power measurements, the benchmark measurements are generally related by common sets of uncertain system parameters. Consequently, the components of the random vector $\mathbf{y}_B(\mathbf{x}_B)$ are generally stochastically dependent, and the covariance matrix $\boldsymbol{\Sigma}_{VB}$ is generally not diagonal.

One way to evaluate the covariance matrix $\boldsymbol{\Sigma}_{VB}$ is via a Monte Carlo method, where we draw a sufficient number of random samples of the system parameter vector $\mathbf{x}_B$, insert them into transport calculations for $\mathbf{y}_B$ and calculate a statistical estimate of $\boldsymbol{\Sigma}_{VB}$ analogous to Eq. (12); see Buss et al. (2010).

Another way to calculate $\boldsymbol{\Sigma}_{VB}$ is via a first order series expansion of $\mathbf{y}_B$ about the nominal system parameter vector $\mathbf{x}_{B,0}$:

$$\begin{aligned} \mathbf{y}_B(\mathbf{x}_B) &\simeq \mathbf{y}_B(\mathbf{x}_{B,0}) + \mathbf{S}_B\left(\mathbf{x}_B - \mathbf{x}_{B,0}\right), \\ (\mathbf{S}_B)_{ij} &= \partial y_{Bi}/\partial x_{Bj}|_{\mathbf{x}_B=\mathbf{x}_{B,0}}, \end{aligned} \quad (13)$$

which is an acceptable approximation if the system parameter uncertainties represented by $\mathrm{p}(\mathbf{x}_B)$ are sufficiently small. The covariance matrix $\boldsymbol{\Sigma}_{VB}$ is then obtained by a linear transformation of the covariance matrix $\boldsymbol{\Sigma}_{\mathbf{X}B}$ of the system parameters $\mathbf{x}_B$ defined by the sensitivity matrix $\mathbf{S}_B$:

$$\boldsymbol{\Sigma}_{VB} \simeq \mathbf{S}_B\boldsymbol{\Sigma}_{\mathbf{X}B}\mathbf{S}_B^T. \quad (14)$$

Having calculated the prior model parameters, $\mathbf{y}_0$ and $\boldsymbol{\Sigma}_0$, and the covariance matrix of the likelihood function $\boldsymbol{\Sigma}_{VB}$, the posterior model parameters, $\mathbf{y}^*$ and $\boldsymbol{\Sigma}^*$, are obtained by minimizing the quadratic form Q^* in Eq. (5) using standard methods of numerical linear algebra.

2.3. The GLLS method as a first-order approximation

If nuclear data uncertainties are sufficiently small, the integral observable vector $\mathbf{y}$ may be approximated by a

first-order series expansion about the best-estimate nuclear data vector $\boldsymbol{\alpha}_0$:

$$\begin{aligned} \mathbf{y}(\boldsymbol{\alpha}) &\simeq \mathbf{y}(\boldsymbol{\alpha}_0) + \mathbf{S}\boldsymbol{\Delta\alpha}, \quad \boldsymbol{\Delta\alpha} = \boldsymbol{\alpha} - \boldsymbol{\alpha}_0, \\ (\mathbf{S})_{ij} &= \partial y_i / \partial \alpha_j |_{\boldsymbol{\alpha}=\boldsymbol{\alpha}_0} . \end{aligned} \tag{15}$$

Choosing a multivariate normal distribution model for the nuclear data vector $\boldsymbol{\alpha}$,

$$\mathrm{p}(\boldsymbol{\alpha}) = \mathrm{N}(\boldsymbol{\alpha}_0, \boldsymbol{\Sigma}_\alpha), \tag{16}$$

the first order expansion yields the following expressions for the distribution model parameters of the prior pdf of $\mathbf{y}$:

$$\begin{aligned} \mathbf{y}_{0A} &\simeq \mathbf{y}_A(\boldsymbol{\alpha}_0), \quad \mathbf{y}_{0B} \simeq \mathbf{y}_B(\boldsymbol{\alpha}_0), \quad \boldsymbol{\Sigma}_{0A} \simeq \mathbf{S}_A \boldsymbol{\Sigma}_\alpha \mathbf{S}_A^T, \\ \boldsymbol{\Sigma}_{0B} &\simeq \mathbf{S}_B \boldsymbol{\Sigma}_\alpha \mathbf{S}_B^T, \quad \boldsymbol{\Sigma}_{0AB} \simeq \mathbf{S}_A \boldsymbol{\Sigma}_\alpha \mathbf{S}_B^T, \end{aligned} \tag{17}$$

cf. Eq. (7). Here $\mathbf{S}_A$ and $\mathbf{S}_B$ denote the application case and benchmark submatrices of the sensitivity matrix $\mathbf{S}$.

Inserting Eq. (17) into Eq. (9) yields the well-known GLLS results of the posterior model parameters (Cecchini et al., 1965; Humi et al., 1965; Hemment and Pendleburry, 1966; Broadhead et al., 2004; De Saint Jean et al., 2011; Salvatores et al., 2013):

$$\begin{aligned} \mathbf{y}_A^* &\simeq \mathbf{y}_{0A} + \mathbf{S}_A \boldsymbol{\Delta\alpha}^*, \quad \mathbf{y}_B^* \simeq \mathbf{y}_{0B} + \mathbf{S}_B \boldsymbol{\Delta\alpha}^*, \\ \boldsymbol{\Sigma}_A^* &\simeq \mathbf{S}_A \boldsymbol{\Sigma}_\alpha^* \mathbf{S}_A^T, \quad \boldsymbol{\Sigma}_B^* \simeq \mathbf{S}_B \boldsymbol{\Sigma}_\alpha^* \mathbf{S}_B^T, \\ \boldsymbol{\Sigma}_{AB}^* &\simeq \mathbf{S}_A \boldsymbol{\Sigma}_\alpha^* \mathbf{S}_B^T. \end{aligned} \tag{18}$$

with

$$\begin{aligned} \boldsymbol{\Delta\alpha}^* &= \boldsymbol{\alpha}^* - \boldsymbol{\alpha}_0 \\ &= \boldsymbol{\Sigma}_\alpha \mathbf{S}_B^T \left(\mathbf{S}_B \boldsymbol{\Sigma}_\alpha \mathbf{S}_B^T + \boldsymbol{\Sigma}_{VB} \right)^{-1} \left(\mathbf{v}_B - \mathbf{y}_{0B} \right), \\ \boldsymbol{\Sigma}_\alpha^* &= \boldsymbol{\Sigma}_\alpha - \boldsymbol{\Sigma}_\alpha \mathbf{S}_B^T \left(\mathbf{S}_B \boldsymbol{\Sigma}_\alpha \mathbf{S}_B^T + \boldsymbol{\Sigma}_{VB} \right)^{-1} \mathbf{S}_B \boldsymbol{\Sigma}_\alpha. \end{aligned} \tag{19}$$

Hence, the GLLS estimates are linear transformations of the maximum-a-posteriori estimate $\boldsymbol{\alpha}^*$ of the nuclear data vector $\boldsymbol{\alpha}$ and of the corresponding posterior nuclear data covariance matrix $\boldsymbol{\Sigma}_\alpha^*$.

At this point, it is important to stress that this linear relationship between integral observables and nuclear data is a result of first-order perturbation theory expressed by Eq. (15). Since Eqs. (18) and (19) represent a first-order approximation of Eq. (9), the GLLS approximation yields acceptable predictions only for sufficiently small nuclear data uncertainties (Hoefer et al., 2011; Rochman et al., 2011b).

3. Applications

3.1. Prediction of the reactivity of a water-moderated fuel assembly

As a first test case of the MOCABA procedure, we choose an exercise from the preliminary Phase IV benchmark specification (Hoefer et al., 2012) for the Expert Group on Uncertainty Analysis for Criticality Safety Analysis (UACSA) of the OECD/NEA Working Party on Nuclear Criticality Safety (WPNCS). This UACSA benchmark was defined with the objective to calculate the Pearson correlations due to system parameter uncertainties between the neutron multiplication factors k_{eff} of experiments belonging to the same series of criticality safety benchmark experiments and to quantify the impact of these correlations on the prediction of the k_{eff} value of an application case; see also Bock and Stuke (2013) and Bock and Behler (2013).

The selected exercise involves 21 criticality safety benchmark experiments from the ICSBEP handbook (NEA Nuclear Science Committee, 2012). Four experiments are taken from LEU-COMP-THERM-007 (Cases 1, 2, 3 and 4) and 17 experiments from LEU-COMP-THERM-039 (all 17 cases). Each of these 21 experimental configurations is defined by a single water-moderated array of fuel rods in a square pitch arrangement. The fuel rods contained low-enriched UO_2 fuel. For each experiment, the fuel rod array was placed in a tank and the water level was raised close to the critical level; see Figure 1. The critical water height was then obtained by extrapolation from the subcritical water height measurements to the critical water height.

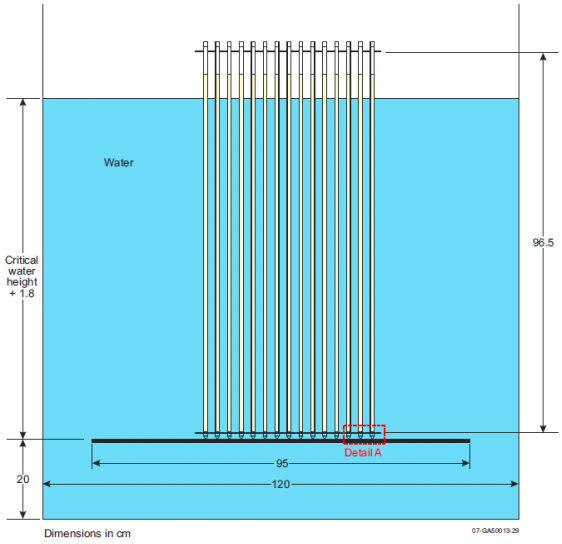

Figure 1: LCT-007/039: Schematic overview of the experimental setup (adopted from NEA Nuclear Science Committee (2012)).

The 21 configurations differ in the number and pattern of fuel rods within the fuel rod array and in the fuel rod pitch which is related to the moderator-to-fuel ratio. All experiments made use of the same experimental equipment and the same fuel rods. To cover the stochastic dependencies between the k_{eff} values of different criticality experiments, a complete stochastic dependence between the fuel rod parameters of different fuel rods is assumed, i.e. all fuel rods are assumed to be characterized by a single parameter

for the fuel rod outer diameter, a single parameter for the fuel density, a single parameter for the U-235 enrichment, etc.

Among the benchmark system parameter uncertainties specified in NEA Nuclear Science Committee (2012), uncertainties in the fuel rod inner diameter, the fuel rod thickness, and the mean linear density of the fuel column have the highest impact on k_{eff}. Hence, these parameters are chosen as the components of the three-dimensional benchmark system parameter vector $\mathbf{x}_B$, and the corresponding 3×3 covariance matrix $\mathbf{\Sigma}_{XB}$ is derived from the uncertainty specification in NEA Nuclear Science Committee (2012). The covariance matrix $\mathbf{\Sigma}_{VB}$ of the likelihood function is calculated from $\mathbf{\Sigma}_{XB}$ according to Eq. (14), where the components of the sensitivity matrix $\mathbf{S}_B$ are derived from SCALE 6.0 criticality calculations for variations of the three system parameters.

As appears from Figure 2, the Pearson correlations due to system parameter uncertainties between the different benchmark k_{eff} values are generally very high. In fact, they are higher than 0.98 except for Case 3 and Case 4 of LCT-007. This is explained by the fact that Case 3 is close to optimum moderation and Case 4 is over-moderated, while the remaining 19 experiments are under-moderated.

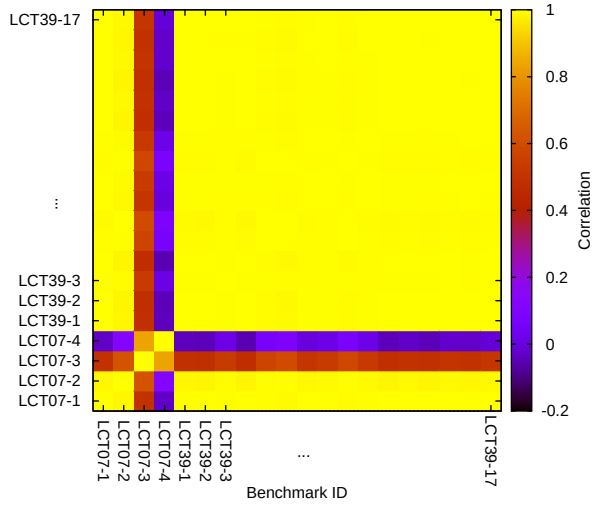

Figure 2: Pearson correlation matrix corresponding to $\mathbf{\Sigma}_{VB}$ for the 21 experiments (Cases 1-4 of LCT-007 and Cases 1-17 of LCT-039).

As an application case, we select from Hoefer et al. (2012) the prediction of the neutron multiplication factor of a PWR fuel assembly which is moderated and fully reflected by pure water; see Figure 3. Uncertainties are specified for six different system parameters, defining the dimensions of the fuel rods, the guide thimbles and the height of the fuel column. These six parameters are identified with the components of the system parameter vector $\mathbf{x}_A$; see Section 2.1. The pdf $\mathrm{p}(\mathbf{x}_A)$ follows directly from the uncertainty specification in Hoefer et al. (2012).

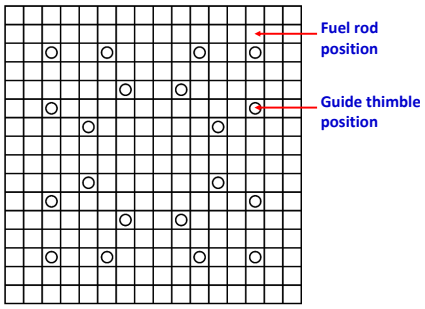

Figure 3: Fuel rod lattice of a 16×16 PWR fuel assembly.

Following the notation of Section 2.1, the components of the 22-dimensional vector $\mathbf{y}$ are given by the k_{eff} values of the application case and the 21 benchmark experiments:

$$\begin{aligned} \mathbf{y} &= (y_1, \ldots, y_{22})^T \\ &= (k_{\text{app}}, k_{\text{LCT}-7-1}, \ldots, k_{\text{LCT}-39-17})^T . \end{aligned} \tag{20}$$

For the calculation of the prior and posterior distribution of $\mathbf{y}$, we follow the MOCABA procedure described in Section 2.2. This evaluation is based on 1000 Monte Carlo samples of the nuclear data for ^{235}U, ^{238}U, ^{1}H and ^{16}O and of the application case system parameters. For the nuclear data sampling the covariance information included in the ENDF/B-VII.1 nuclear data evaluation (Chadwick et al., 2011) is used. The criticality calculations are performed with SCALE 6.0 using 44-group nuclear data libraries (Oak Ridge National Laboratory, 2009).

Figure 4 shows the mean values for the prior and posterior distributions of the benchmark experiments. One observes a sizable bias in the prior k_{eff} distributions which is predominantly caused by the procedure chosen to collapse the point-wise ENDF/B 7.1 nuclear data to the 44-group SCALE input library. The 44-group libraries provided by ORNL as part of its SCALE Oak Ridge National Laboratory (2009) package are generated in a two-step process, where first a 238-group library is generated which is then collapsed to 44 groups based on a PWR-like spectrum. In this work, the collapsing was performed in a one-step procedure using a spectrum that represents a combination of a $1/E$, a fission, and a thermal Maxwellian spectrum (NJOY option IWT=4). MOCABA corrects the bias induced by the simplified group collapsing scheme, and thus shifts the posterior distribution towards larger k_{eff} values. More recent NUDUNA applications are based on 238-group libraries and show for low-enriched UO_2 and MOX lattices moderated by water similar prior biases as default SCALE libraries.

The evaluation of the prior covariance matrix $\mathbf{\Sigma}_0$ according to Eq. (12) reveals high correlations due to nuclear

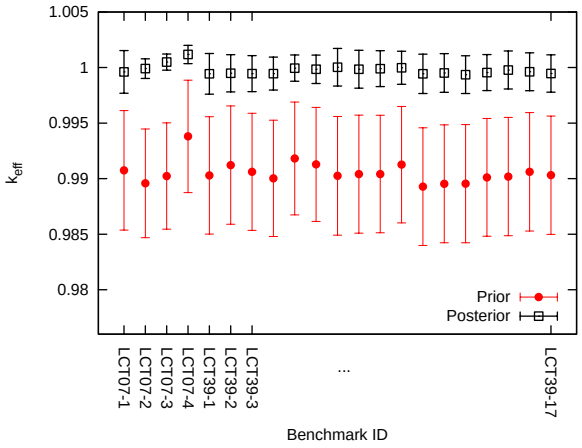

Figure 4: Mean values of the prior and posterior k_{eff} distributions for the 21 benchmark experiments. The error bars show the standard deviations of the distributions.

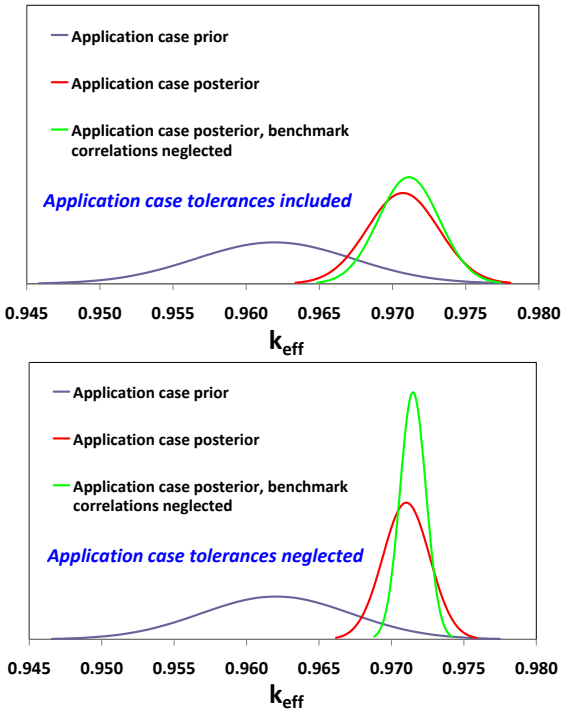

Figure 5: Prior and posterior k_{eff} distribution for the application case. For the lower panel, the system parameter uncertainties of the application case were neglected, i.e. the application case system parameter vector $\mathbf{x}_A$ was kept constant at its nominal value (no Monte Carlo sampling of $\mathbf{x}_A$, see Section 2.2).

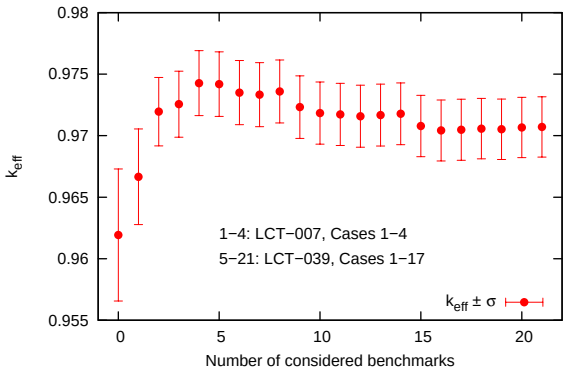

Figure 6: Posterior $k_{\text{eff}} \pm \sigma$ for the application case as a function of the number of benchmark experiments taken into account in the Bayesian updating procedure.

data uncertainties between the k_{eff} values of the benchmark experiments and of the application case. In fact, these correlations are higher than 0.97 except for Case 3 and Case 4 of LCT-007. Hence, we may expect that our knowledge about the application case k_{eff} value will be significantly improved by taking into account the benchmark experiments.

This expectation is confirmed by Figure 5, since the width of the posterior distribution is significantly reduced compared to the width of the prior distribution. As also appears from this figure, covariances due to system parameter uncertainties between the k_{eff} values of different benchmark experiments enhance the width of the posterior k_{eff} distribution which reflects a decrease in information. Hence, it is generally important to take covariances due to system parameter uncertainties into account.

Figure 6 shows the posterior $k_{\text{eff}} \pm \sigma$ values of the application case as a function of the number of benchmark experiments taken into account. As can be seen, the posterior k_{eff} predictions become nearly stable after the first five benchmark experiments have been added, and the posterior uncertainty is not further reduced. The reason is, as follows from Figure 5, that after adding the first 5 benchmark experiments the posterior uncertainty is dominated by the application case tolerances, and this uncertainty cannot be reduced by adding more benchmark information.

3.2. Power distribution of a toy model reactor

The example presented in the last sub-section was related to the prediction of a single integral observable, namely the neutron multiplication factor of a water-moderated fuel assembly, where the integral observable vector $\mathbf{y}_A$ of the application case had only one component. Since MOCABA may be applied to the prediction of any vector function of a nuclear data vector $\boldsymbol{\alpha}$, we are now going to test the updating algorithm of MOCABA for a simple reactor toy model where $\mathbf{y}_A$ has dimension 100. The purpose of this toy model, which is similar to the one used for an exercise in Hoefer et al. (2012), is not to simulate a real reactor core but to demonstrate the MOCABA method for a high-dimensional integral vector function.

Each component of $\mathbf{y}_A$ may be thought of as the thermal power of one out of 100 fuel assemblies within a nu-

clear reactor. Hence, the sum of the components of $\mathbf{y}_A$ represents the total reactor power.

We assume a four-dimensional nuclear data random vector $\boldsymbol{\alpha}$ defined by the following pdf:

$$\begin{aligned} \mathrm{p}(\boldsymbol{\alpha}) &= \mathrm{N}(\boldsymbol{\alpha}_0, \boldsymbol{\Sigma}_\alpha), \\ \boldsymbol{\alpha}_0 &= (9.9968, 1.0066, 1.0225, 1.2198)^T, \\ \boldsymbol{\Sigma}_\alpha &= \mathbf{diag}\,(0.3, 0.03, 0.03, 0.03)\ . \end{aligned} \tag{21}$$

$\mathbf{y}_A$ is supposed to be given by the following vector function:

$$\begin{aligned} \mathbf{y}_A &= (y_{A,1}, \ldots, y_{A,100})^T, \quad y_{A,i} = \boldsymbol{\alpha}^T \mathbf{x}_{A,i}, \\ \mathrm{p}(\mathbf{x}_{A,i}) &= \mathrm{N}\left(\mathbf{x}_{A,0}, \boldsymbol{\Sigma}_{XA}\right), \quad \mathbf{x}_{A,0} = (0.6, 6, -12, 24)^T, \\ \boldsymbol{\Sigma}_{XA} &= \mathbf{diag}\,(0.006, 0.06, 0.12, 0.24)\,. \end{aligned} \tag{22}$$

We further assume nine benchmark measurements being related to the following vector function:

$$\begin{aligned} \mathbf{y}_B &= (y_{B,1}, \ldots, y_{B,9})^T, \\ y_{B,i} &= \frac{\alpha_1 \alpha_4 x_{B1}}{\alpha_1 x_{B1} + \alpha_2 x_{B2}^{(i)} + \alpha_3 x_{B3}^{(i)}}. \end{aligned} \tag{23}$$

The components $y_{B,i}$ of $\mathbf{y}_B$ may be thought of as neutron multiplication factors of nine different critical configurations, i.e. the measurements of $y_{B,i}$ are given by $v_{B,i} = 1$, and the uncertainty distributions of the benchmark system parameters follow directly from Table 1, where we assume normal distribution models for all system parameters.

The second to last column in Table 1 contains the calculated benchmark k_{eff} values $y_{B,i}^{(0)}$ for the nominal values of the nuclear data and the benchmark system parameters.

The observed Pearson correlations due to nuclear data uncertainties between the elements of the application case vector $\mathbf{y}_A$ and the benchmark vector $\mathbf{y}_B$, corresponding to the submatrix $\boldsymbol{\Sigma}_{0AB}$ of $\boldsymbol{\Sigma}_0$ (see Eq. (7)), are in the range between 0.7 and 0.93. Hence, we may expect that taking into account the benchmark measurements will significantly improve our knowledge about $\mathbf{y}_A$.

This expectation is confirmed by Figure 7, which shows the prior and posterior pdfs of the total reactor power, i.e. the sum of all 100 components of $\mathbf{y}_A$, and of the power $y_{A,i}$ of a single fuel assembly. As can be seen, the widths of the posterior distributions are much smaller than those of the prior distributions, which reflects a strong increase in information. Here the posterior distributions are presented for three different cases: the green curves correspond to the case where no constraints are imposed on the total reactor power, the blue curves correspond to a total power of 2900 MW with a standard deviation of 10 MW, and the red curves correspond to a total power of exactly 2900 MW.[3]

[3]It should be noted that for a real reactor power simulation the total power is fixed, i.e. the power distribution is normalized to the total power. This means that the sum constraint has to be applied already to the prior local power vector $\mathbf{y}$ before taking into account any measurements. According to Section 2.1, within the MOCABA framework this sum constraint (as a special case of a linear constraint) is imposed by means of Bayesian updating of the unconstrained prior pdf of $\mathbf{y}$. Information from benchmark measurements can then be included in a second updating step. For the considered toy model this two-step updating procedure, which is mathematically equivalent to a single combined updating step, yields the red curves shown in Figure 7 if the total power is constrained to be 2900 MW.

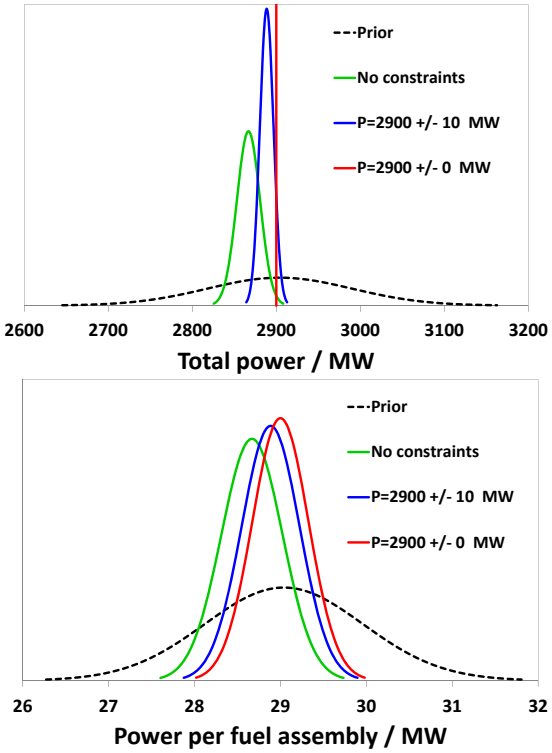

Figure 7: Prior and posterior distributions for total reactor power and power per fuel assembly.

Predicting the power distribution for a real reactor core would follow a similar procedure as for the toy model example, except that one would use NUDUNA for the nuclear data sampling, and the analytic expressions in Eqs. (22) and (23) would be replaced by transport calculation results.

4. Conclusions

MOCABA combines the advantages of Monte Carlo based nuclear data uncertainty propagation (no first order approximation, no adjoint calculations necessary, applicable to any function of nuclear data) with those of the Generalized Linear Least Squares method (updating of predictions of integral observables by taking into account integral measurements). Being based on a general Bayesian scheme, MOCABA can be applied to the prediction of any kind of integral observable (neutron multiplication factors, isotopic concentrations in irradiated nuclear fuel, reactor

Table 1: System parameters defining the 9 benchmark experiments.

Benchmark i	x_{B1}	σ_{B1}	$x_{B2}^{(i)}$	$\sigma_{B2}^{(i)}$	$x_{B3}^{(i)}$	$\sigma_{B3}^{(i)}$	$y_{B,i}^{(0)}$	$v_{B,i}$
1	2.0072	0.05	4.0424	0.05	-0.0746	0.05	1.0174	1.0
2	2.0072	0.05	1.9601	0.05	1.9292	0.05	1.0194	1.0
3	2.0072	0.05	-0.0506	0.05	3.9477	0.05	1.0177	1.0
4	2.0072	0.05	-2.0458	0.05	6.0650	0.05	1.0111	1.0
5	2.0072	0.05	-3.9905	0.05	8.0370	0.05	1.0086	1.0
6	2.0072	0.05	-6.0613	0.05	9.8448	0.05	1.0185	1.0
7	2.0072	0.05	-12.0059	0.05	15.9819	0.05	1.0063	1.0
8	2.0072	0.05	-16.0923	0.05	19.9995	0.05	1.0066	1.0
9	2.0072	0.05	-20.0440	0.05	23.9692	0.05	1.0032	1.0

power distributions, etc.), and any integral measurement may be used as a benchmark to update the prediction of an integral observable. Additionally, constraints on linear combinations of integral observables can be accounted for, e.g. a constraint on the total reactor power for the prediction of a reactor power distribution. MOCABA incorporates the NUDUNA code for the nuclear data sampling. Since NUDUNA performs its sampling directly on evaluated nuclear data files in ENDF-6 format, the MOCABA procedure is not restricted to any particular nuclear data library format of a transport code system. The current NUDUNA version supports automatic compilation of ACE and AMPX libraries, i.e. MOCABA can already be used in combination with continuous energy MCNP or SERPENT transport calculations and multigroup SCALE calculations. A NUDUNA upgrade for generating few-group libraries for reactor core simulation systems is in development, so that the MOCABA code system will also be applicable to reactor core design and reactor safety analysis.

Acknowledgements

This work was conducted in the framework of the AREVA GmbH R&D project "Uncertainty Analysis and Uncertainty Propagation in Nuclear Design Systems"'. We thank M. Lamm for his support in R&D project management.

References

Bock, M., Behler, M., 2013. Impact of correlated benchmark experiments on the computational bias in criticality safety assessment. In: Proc. ANS Nuclear Criticality Safety Division Topical Meeting (NCSD 2013). Wilmington, North Carolina, USA.

Bock, M., Stuke, M., 2013. Determination of correlations among benchmark experiments by Monte Carlo sampling techniques. In: Proc. ANS Nuclear Criticality Safety Division Topical Meeting (NCSD 2013). Wilmington, North Carolina, USA.

Broadhead, B., Rearden, B., C.M., H., Wagschal, J., Parks, C., 2004. Sensitivity- and uncertainty-based criticality safety validation techniques. Nucl. Sci. Eng. 146, 340–366.

Buss, O., Hoefer, A., Neuber, J., 2010. Hierarchical Monte Carlo approach to bias estimation for criticality safety calculations. In: Proc. Physics of Reactors International Conference (PHYSOR 2010). Pittsburgh, Pennsilvania, USA.

Buss, O., Hoefer, A., Neuber, J., 2011. NUDUNA - nuclear data uncertainty analysis. In: Proc. International Conference on Nuclear Criticality (ICNC 2011). Edinburgh, Scotland.

Cecchini, G., Farinelli, U., Gandini, A., Salvatores, M., 1965. Analysis of integral data for few-group parameter evaluation of fast reactors. In: Proc. of the 3rd International Conference on Peaceful Uses of Atomic Energy. New York, USA.

Chadwick, M., Herman, M., Obložinský, P., Dunn, M., Danon, Y., Kahler, A., Smith, D., Pritychenko, B., Arbanas, G., Arcilla, R., Brewer, R., Brown, D., Capote, R., Carlson, A., Cho, Y., Derrien, H., Guber, K., Hale, G., Hoblit, S., Holloway, S., Johnson, T., Kawano, T., Kiedrowski, B., Kim, H., Kunieda, S., Larson, N., Leal, L., Lestone, J., Little, R., McCutchan, E., MacFarlane, R., MacInnes, M., Mattoon, C., McKnight, R., Mughabghab, S., Nobre, G., Palmiotti, G., Palumbo, A., Pigni, M., Pronyaev, V., Sayer, R., Sonzogni, A., Summers, N., Talou, P., Thompson, I., Trkov, A., Vogt, R., van der Marck, S., Wallner, A., White, M., Wiarda, D., Young, P., 2011. ENDF/B-VII.1 Nuclear Data for Science and Technology: Cross Sections, Covariances, Fission Product Yields and Decay Data. Nuclear Data Sheets 112 (12), 2887–2996.

CSEWG, Jul. 2013. ENDF-6 Formats Manual. Data Formats and Procedures for the Evaluated Nuclear Data Files ENDF/B-VI and ENDF/B-VII. CSEWG Document ENDF-102 BNL-90365-2009 Rev.1, Brookhaven National Laboratory, Upton, USA.

De Saint Jean, C., Dupont, E., Ishikawa, M., Palmiotti, G., Salvatores, M., 2011. Assessment of existing nuclear data adjustment methodologies. NEA/NSC/WPEC/DOC(2010)429.

Diez, C., Cabellos, O., Rochman, D., Koning, A., Martinez, J., 2013. Monte Carlo uncertainty propagation approaches in ADS burn-up calculations. Ann. Nucl. Energy 54, 27–35.

Gandini, A., 1967. A generalized perturbation method for bilinear functionals of the real and adjoint neutron fluxes. J. Nucl. Energy 21, 755.

Garcia-Herranz, N., Cabellos, O., Sanz, J., Juan, J., Kuijper, J., 2008. Propagation of statistical and nuclear uncertainties in Monte Carlo burn-up calculations. Ann. Nucl. Energy 35, 714–730.

Gelman, A., Carlin, J., Stern, H., Rubin, D., 1998. Bayesian data analysis, second edition. Chapman & Hall/CRC.

Hemment, P., Pendleburry, E., 1966. The optimization of neutron cross-section data adjustments to give agreement with experimental critical size. In: Proc. Int. Conf. on Fast Critical Experiments and Their Analysis. ANL, Illinois.

Hoefer, A., Buss, O., Neuber, J., 2011. How confident can we be in confidence intervals for the computational bias obtained with the generalized linear least squares methodology? - a toy model analysis. In: Proc. International Conference on Nuclear Criticality (ICNC 2011). Edinburgh, Scotland.

Hoefer, A., Ivanova, T., Rearden, B., 2012. Proposal for an UACSA Phase IV benchmark on correlations between criticality safety

benchmark experiments. Meeting of the UACSA Expert Group, OECD/NEA, Paris, France.

Humi, M., Wagschal, J., Yeivin, Y., 1965. Multi-group constants from integral data. In: Proc. of the 3rd International Conference on Peaceful Uses of Atomic Energy. New York, USA.

JEFF team, 2014. JEFF-3.2: Evaluated data library. URL http://www.oecd-nea.org/dbforms/data/eva/evatapes/jeff_32/

Klein, M., Gallner, L., Krzykacz-Hausmann, B., Pautz, A., Velkov, K., Zwermann, W., 2012. Interaction of loading pattern and nuclear data uncertainties in reactor core calculations. In: Proc. Physics of Reactors International Conference (PHYSOR 2012). Knoxville, Tennessee, USA.

Koning, A., Rochman, D., 2008. Towards sustainable nuclear energy: Putting nuclear physics to work. Ann. Nucl. Energy 35, 2024–2030.

Koning, A., Rochman, D., 2011. Modern nuclear data evaluation with the TALYS code system. Nuclear Data Sheets 113 (12), 2841–2934.

Leppänen, J., 2013. Serpent - a continuous-energy Monte Carlo reactor physics burnup calculation code. User's Manual, VTT Technical Research Centre of Finland. URL http://montecarlo.vtt.fi/download/Serpent_manual.pdf

NEA Nuclear Science Committee, 2012. International handbook of evaluated criticality safety benchmark experiments. NEA/NSC/DOC(95)03.

Oak Ridge National Laboratory, January 2009. SCALE: A Modular Code System for Performing Standardized Computer Analysis for Licensing Evaluation, ORNL/TM-2005/39, Version 6.0. Oak Ridge, Tennessee, USA.

Pasichnyk, I., Klein, M., Velkov, K., Zwermann, W., Pautz, A., 2012. Nuclear data uncertainties by the PWR MOX/UO2 core rod ejection benchmark. In: Proc. Physics of Reactors International Conference (PHYSOR 2012). Knoxville, Tennessee, USA.

Rochman, D., Koning, A., van der Mark, S., 2011a. Exact nuclear data uncertainty propagation for fusion design. J. Korean Phys. Soc. 59 (2), 1386–1389.

Rochman, D., Koning, A., van der Mark, S., Hogenbirk, A., Sciolla, C., 2011b. Nuclear data uncertainty propagation: Perturbation vs. Monte Carlo. Ann. Nucl. Energy 38, 942–952.

Salvatores, M., Palmiotti, G., Aliberti, G., McKnight, R., Archier, P., De Saint-Jean, C., Dupont, E., Herman, M., Ishikawa, M., Sugino, K., Ivanova, T., Ivanov, E., Kim, S.-J., Kodeli, I., Trkov, A., Manturov, G., Pelloni, S., Perfetti, C., Rearden, B., Plompen, A., Rochman, D., Wang, W., Wu, H., Yang, W., 2013. Methods and issues for the combined use of integral experiments and covariance data. NEA/NSC/WPEC/DOC(2013)445.

Sanz, J., Cabellos, O., Garcia-Herranz, N., 2008. ACAB-2008: Activation abacus code. NEA Data Bank, NEA-1839 ACAB 2008.

Shibata, K., Iwamoto, O., Nakagawa, T., Iwamoto, N., Ichihara, A., Kunieda, S., Chiba, S., Furutaka, K., Otuka, N., Ohasawa, T., Murata, T., Matsunobu, H., Zukeran, A., Kamada, S., Katakura, J.-I., 2011. JENDL-4.0: A New Library for Nuclear Science and Engineering. Journal of Nuclear Science and Technology 48 (1), 1–30.

Uchasev, L., 1964. Perturbation theory for the breeding ratio and other number ratios pertaining to various reactor processes. J. Nucl. Energy, Part A/B 18, 571.

Wieselquist, W., Zhu, T., Vasiliev, A., Ferroukhi, H., 2013. PSI methodologies for nuclear data uncertainty propagation with CASMO-5M and MCNPX: Results for OECD/NEA UAM benchmark Phase I. Sci. Technol. Nucl. Install. 2013.

Williams, M., Wiarda, D., Smith, H., Jessee, M., Rearden, B., Zwermann, W., Klein, M., Pautz, A., Krzykacz-Hausmann, B., Gallner, L., 2012. Development of a statistical sampling method for uncertainty analysis with SCALE. In: Proc. Physics of Reactors International Conference (PHYSOR 2012). Knoxville, Tennessee, USA.

X-5 Monte Carlo Team, Apr. 2003. MCNP – A General Monte Carlo N-Particle Transport Code, LA-CP-03-0245, Version 5. Los Alamos, New Mexico, USA.

Zwermann, W., Krzykacz-Hausmann, B., Gallner, L., Pautz, A., 2010. Uncertainty analyses with nuclear covariance data in reactor core calculations. In: Proc. Jahrestagung Kerntechnik. Berlin, Germany.